Supplementary Information

"Space-time signatures of surface warming accelerations since 1970"

Contents

1 Globally averaged data

We analyze global mean surface temperatures (GMST) over the full record (Figure S1). An acceleration post 1970 is not detected, a result similar to Beaulieu et al. (2024) in which data was analyzed until 2023. We note that the results remain the same with the reduced penalty described in Equation 2 below.

The following GMST datasets were included here:

The Hadley Centre/Climatic Research Unit, Version 5 (HadCRUT), surface temperature (Morice et al., 2021). This series is available at `https://www.metoffice.gov.uk/hadobs/hadcrut5/data/HadCRUT.5.0.2.0/download.html`.

The Merged Land–Ocean Surface Temperature Analysis from the National Oceanic and Atmospheric Administration (NOAAGlobalTemp v6) of Vose et al. (2021). This series is available at `https://www.ncei.noaa.gov/data/noaa-global-surface-temperature/v6/access/timeseries/`.

The Berkeley Earth Surface Temperatures (Berkeley) of Rohde and Hausfather (2020). This series is available at `http://berkeleyearth.org/data`.

The Goddard Institute for Space Studies (GISS) Surface Temperature Analysis (GISTEMP) at the National Aeronautic Space Administration (NASA) (Lenssen et al., 2019). This series

is available at `https://data.giss.nasa.gov/gistemp/`.

Dynamically Consistent ENsemble of Temperature (DCENT) (Chan et al., 2024b,a). This series is available at `https://duochanatharvard.github.io/research_01_DCENT.html`.

Anomalies are computed relative to the period 1850-1900.

2 Additional method considerations

2.1 Reduced penalty

In the main, we analyzed the gridded temperature datasets with a BIC penalty:

$$P(m) = (4m + 4)\ln(N), \tag{1}$$

where m represents the number of changepoints and N is the length of the time series. Here, we also include an analysis on the Berkeley dataset with a reduced penalty:

$$P(m) = (3m + 4)\ln(N), \tag{2}$$

This penalty is less conservative than the BIC penalty used in the main paper 1 and consequently lead to more changes detected. We use this reduced penalty instead of an Akaike Information Criterion (AIC) penalty because the AIC is inconsistent in changepoint settings Zheng et al. (2022). The regional changes identified in the Berkeley surface temperature dataset are presented in Figure S2. With a reduced penalty, the main regions identified in Figures 1-2 in the Main expand and new regions appear that were negligible with a higher penalty.

2.2 False positive rates

To assess the falso positive rates of our changepoint detection technique, we generated 1000 random synthetic series of 55 data points (covering 1970-2024) from a first-order autocorrelation (AR(1)) process

$$\epsilon_t = \phi\epsilon_{t-1} + Z_t, \tag{3}$$

where $\{Z_t\}$ is independent and identically distributed Gaussian noise with a mean of 0 and variance $\sigma^2 = 0.01$ and $\phi = 0.23$. A long-term trend of 0.02 ^oC per year was superimposed. Those values were obtained from the Berkeley global mean surface temperature time series. We analyzed the synthetic time series using a BIC penalty as used in the main (Equation 1) and a reduced penalty included above (Equation 2). Table S1 presents the rate of false detections obtained with both penalties. With the BIC penalty, the false positives rate is smaller as expected.

2.3 True positive rates

To assess the detection power of the changepoint technique, we generated random synthetic series of 55 data points from a first-order autocorrelation (AR(1)) process as in Equation 3 with with a mean of 0 and variance $\sigma^2 = 0.01$ and $\phi = 0.23$, with a superimposed long-term trend of 0.02 ^oC per year. Then, we impose changepoints at times 10, 20, 30 and 40, corresponding to the start of a new regime at years 1980, 1990, 2000 and 2010, representing the different timings detected on gridded surface temperature data. The magnitude of the changepoints is set to vary to represent the range of SNR observed on the surface temperature datasets (Table 1 in the Main) with SNR varying from 0.25 (small SNR, difficult to detect) to 3 (large SNR, easy to detect). We analyze the time series generated with our changepoint model and compute the proportion of time series for which a change in trend is detected when a change is present. The results are presented in Figure S3. For a fixed SNR, the power is slightly higher when the changepoint is closer to the middle of the time series and decreases if the changepoint moves towards the beginning or end of the time series. As such, changes that took place in the 1990s and 2000s are easier to detect than in the 2010s or 1980s. The detection power of the technique utilized here increases rapidly with the SNR: changes with an SNR of 0.5 will likely be detected (probability > 0.75) except if they occur in 1980, then there is a reduced detection power (Figure S3A). With the reduced penalty, the power of detection increases as expected. Changes with a SNR of 0.5 will most likely be detected (probability > 0.9) except if they occurred in 1980 when the power is reduced (Figure S3B). Overall, this power analysis demonstrates the skill of the method used here in detecting a change in trend when there is one.

2.4 Quadratic trend

An alternative representation for an acceleration in warming is a quadratic trend model Richardson (2022). Here we also analyze a gridded surface temperature dataset with a quadratic regression model fitted over the period 1970-2024:

$$X_t = \alpha_1 + \beta_1 t + \beta_2 t^2 + \epsilon_t, \tag{4}$$

where α_1 is the intercept, β_1 and β_2 represent the linear and quadratic trend components and ϵ_t is the errors that we model with a first-order autocorrelation model.

Figure S4 presents the estimates and significance of quadratic trends. Regions identified by the changepoint detection method applied to the Berkeley dataset in Figures 1A and 2A are also flagged here. However, with the quadratic trend there are more grid cells with a detected acceleration than with the piecewise model with a BIC penalty used in the Main. We note that there is no need to estimate the timing of a trend change with the quadratic trend definition, so different results are to be expected. The results obtained in Figure S4 are more in line with the changes detected with a piecewise model and a reduced penalty presented in Figure S2.

References

Beaulieu, C., Gallagher, C., Killick, R., Lund, R., and Shi, X. (2024). A recent surge in global warming is not detectable yet. *Communications Earth & Environment*, 5:576.

Chan, D., Gebbie, G., Huybers, P., and Kent, E. (2024a). DCENT: Dynamically Consistent ENsemble of Temperature at the earth surface. Dataset accessed 2025-05-21.

Chan, D., Gebbie, G., Huybers, P., and Kent, E. C. (2024b). A dynamically consistent ensemble of temperature at the earth surface since 1850 from the dcent dataset. *Scientific Data*, 11.

Lenssen, N. J. L., Schmidt, G. A., Hansen, J. E., Menne, M. J., Persin, A., Ruedy, R., and Zyss, D. (2019). Improvements in the GISTEMP uncertainty model. *Journal of Geophysical Research: Atmospheres*, 124(12):6307–6326.

Morice, C. P., Kennedy, J. J., Rayner, N. A., Winn, J. P., Hogan, E., Killick, R. E., Dunn, R. J. H., Osborn, T. J., Jones, P. D., and Simpson, I. R. (2021). An updated assessment of near-surface temperature change from 1850: The HadCRUT5 data set. *Journal of Geophysical Research: Atmospheres*, 126(3):e2019JD032361.

Richardson, M. T. (2022). Prospects for detecting accelerated global warming. *Geophysical Research Letters*, 49(2):e2021GL095782.

Rohde, R. A. and Hausfather, Z. (2020). The Berkeley Earth land/ocean temperature record. *Earth System Science Data*, 12(4):3469–3479.

Vose, R. S., Huang, B., Yin, X., Arndt, D., Easterling, D. R., Lawrimore, J. H., Menne, M. J., Sanchez-Lugo, A., and Zhang, H. M. (2021). Implementing full spatial coverage in NOAA's global temperature analysis. *Geophysical Research Letters*, 48(4):e2020GL090873.

Zheng, C., Eckley, I., and Fearnhead, P. (2022). Consistency of a range of penalised cost approaches for detecting multiple changepoints. *Electronic Journal of Statistics*, 16:4497–4546.

Tables

Table S1: False positive rates (%) obtained by applying the changepoint technique to 1000 random time series with two different penalties.

Penalty	Rate of false detection (%)
(4m+4)ln(N)	1.8
(3m+4)ln(N)	9.4

Figures

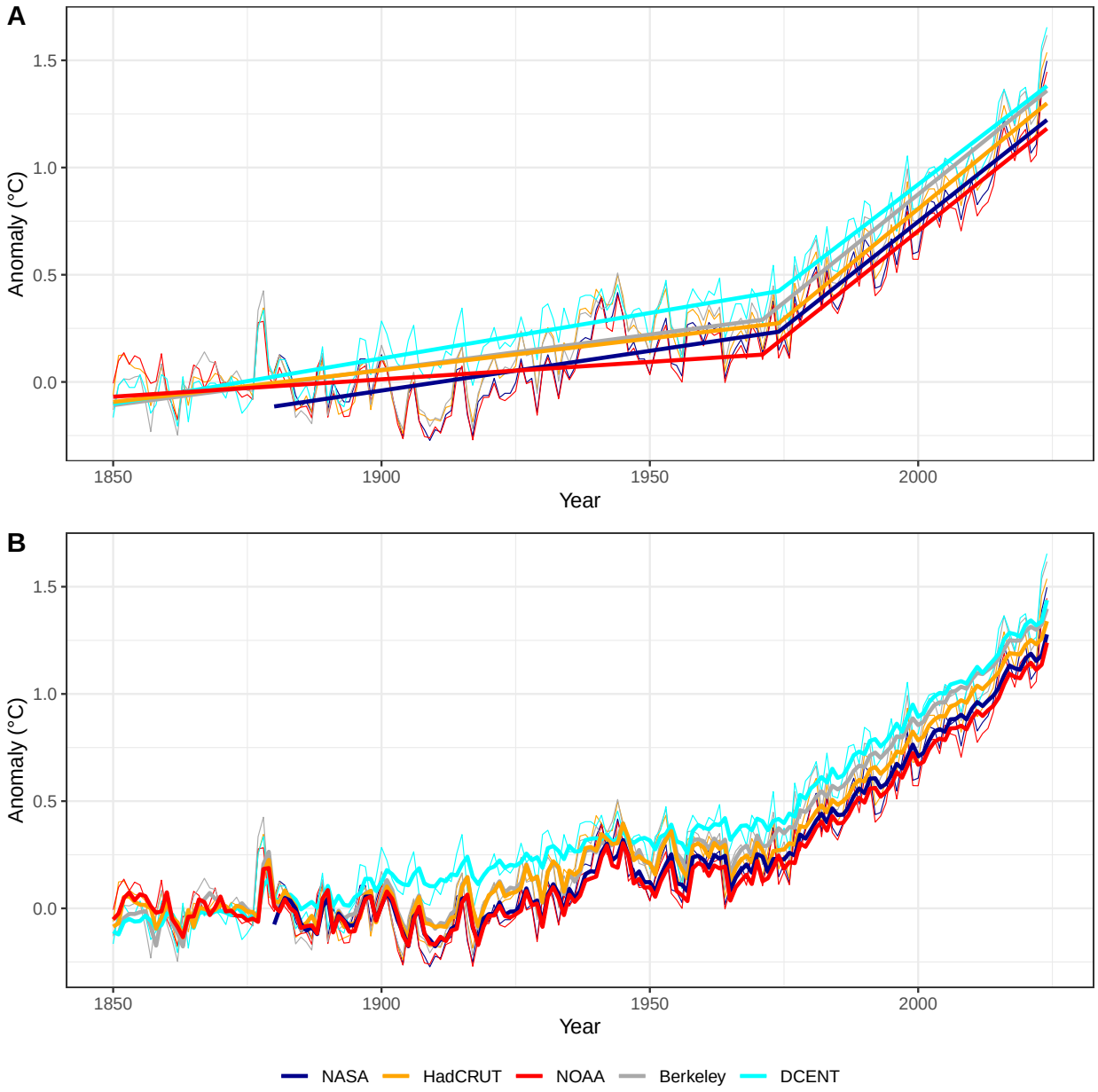

Figure S1: The NASA, HadCRUT, NOAA, Berkeley and DCENT series from 1850-2024 averaged globally. Piecewise linear regression fits are superimposed and showing A) Trend only and B) Trend and autocorrelation.

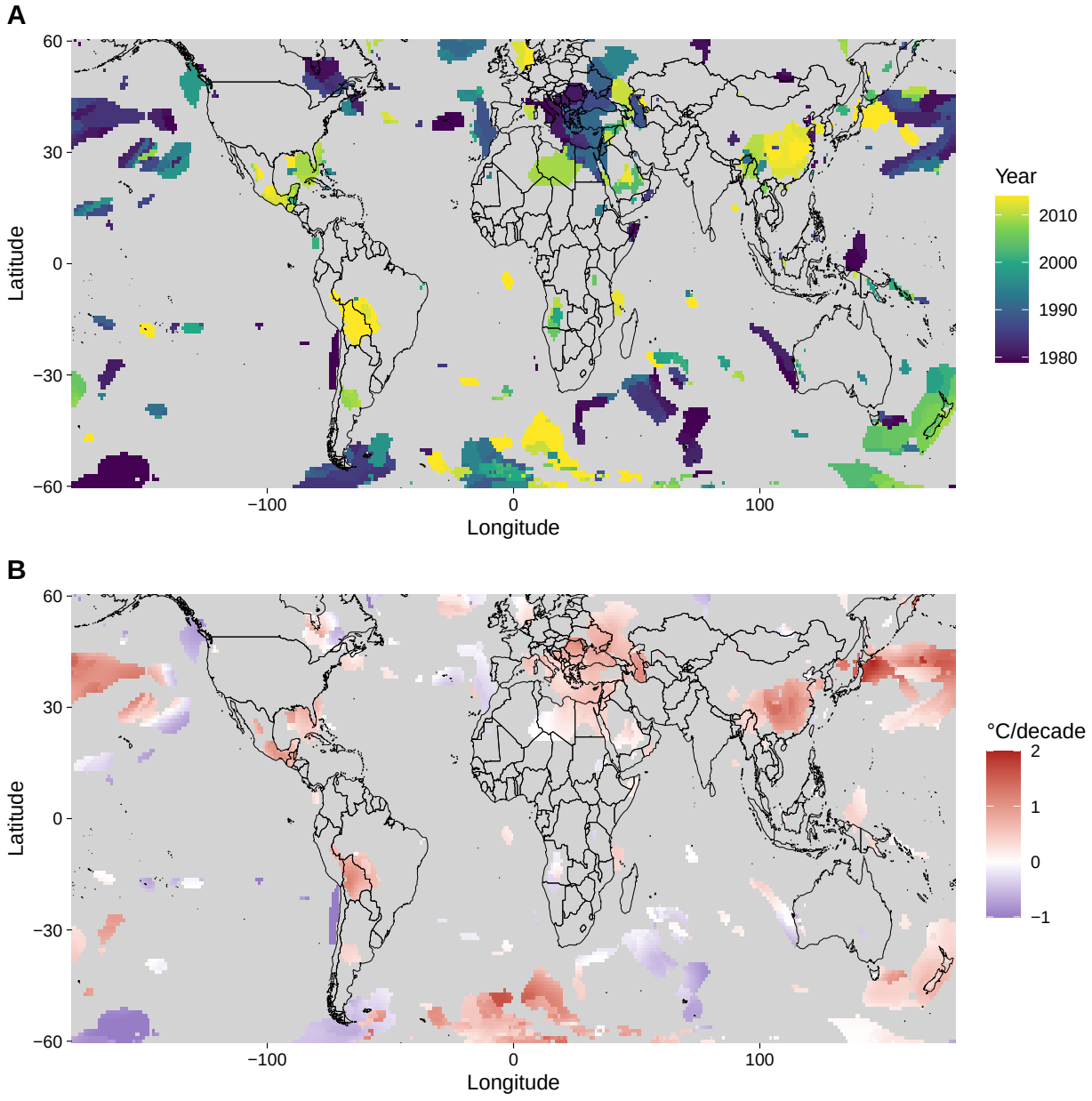

Figure S2: Regional changes in the rate of warming since 1970 detected with a reduced penalty and using the Berkeley dataset. A) Timings of changes detected and B) Magnitude of changes detected. Grey areas indicate where changes are not detectable (or missing data).

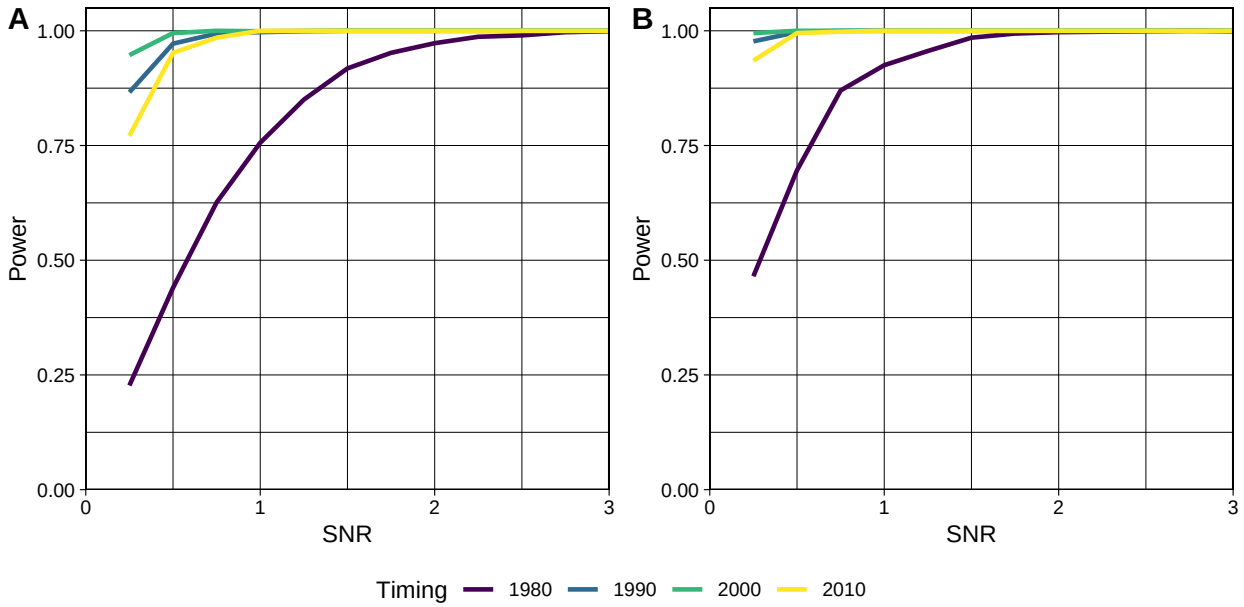

Figure S3: True positive rates of the changepoint detection technique A) with a BIC penalty Equation (4m+4)ln(N) and B) with a reduced penalty (3m+4)ln(N). Note that the false positives are presented in Table S1.

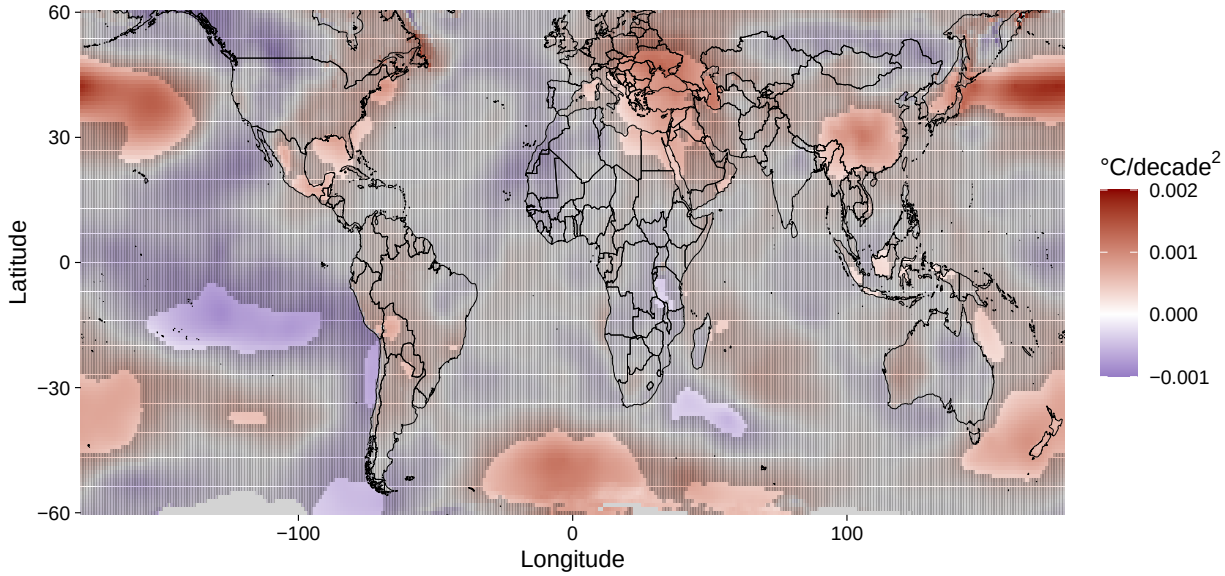

Figure S4: Accelerations in the rate of warming since 1970 represented by a quadratic trend. Stipling indicates where the quadratic trend component is not significantly different from zero (p-value > 0.05).